ACS OMEGA

http://pubs.acs.org/journal/acsodf

Article

Composition, Origin, and Accumulation Model of Coalbed Methane in the Panxie Coal Mining Area, Anhui Province, China

Qiang Wei,* Baolin Hu,* Huihuang Fang,* Song Chen, Songbao Feng, Cancan Wu, and Chunshan Zheng

Cite This: *ACS Omega* 2022, 7, 17929−17940

Read Online

ACCESS | Metrics & More | Article Recommendations

ABSTRACT: To investigate the geochemical characteristic, genetic types, and accumulation model of coalbed methane (CBM), 16 samples from a burial depth of 621−1494 m were collected in the Panxie Coal Mining Area of Huainan Coalfield. The results indicate that the samples are dominated by methane, and the concentrations are distributed in the range of 73.11−95.42%. The dryness coefficient is 0.77−1.00 (average, 0.93), and the ratio of methane to the sum of ethane and propane ($C_1/(C_2 + C_3)$) is 3.18−242.64 (average, 36.15). The $\delta^{13}C_{CH_4}$ values are distributed in the range of −65.44 to −32.38‰ (average, −45.22‰), the δD_{CH_4} values are in the range of −226.84 to −156.82‰ (average, −182.93‰), and the $\delta^{13}C_{CO_2}$ values are in the range of −19.7 to −10.1‰ (average, −15.51‰). CBM samples in the study area are dominated by thermogenic gases, followed by secondary biogenic gases with CO_2 reduction. For the percentages of different genetic gases, the distribution range of thermogenic gas is 70.11−97.86%, whereas that of biogenic gas is 58.65−77.86% for five samples from Zhangji, Panyi, Pansan, and Panbei Coalmines. Moreover, desorption-diffusion fractionation and the effect of groundwater dissolution occurred in the Panxie Coal Mining Area, and higher $\delta^{13}C_{CH_4}$ values mostly existed in the deeper coal seams. Furthermore, the biogenic gases are more likely to be secondary biogenic gases generated by CO_2 reduction on the basis of data comparison, which is related to the flowing water underground. Accumulation models of different genetic types of CBM are correlated with the burial depth of coal seams, location, and type of faults and aquifers.

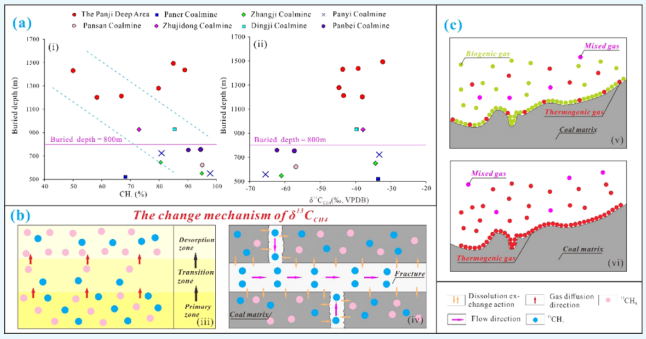

1. INTRODUCTION

As a type of unconventional natural gas, coalbed methane (CBM) resource is abundant in China with successful development.[1,2] In China, the CBM resource at a burial depth of <2000 m is 36.8 × 10^{12} m^3, and that at a burial depth of 1000−2000 m is ∼22.08 × 10^{12} m^3.[3,4] In recent years, China has built several large-scale CBM industrial bases with the Qinshui Basin and the eastern margin of the Ordos Basin as key areas and has a profound understanding of the exploration, development, and production of CBM.[5−8] The Panxie Coal Mining Area with significant coal and CBM resources is located in the eastern part of the Huainan Coalfield, north Anhui Province of China.[9,10] According to the exploration data, an important discovery has been made in the "Panqi-1 well" of the Panxie Coal Mining Area.[11] The tested gas content of shale and coal seam is ∼10 m^3/ton, and the daily gas production of the test well in the Xinxie-1 block located in the south of Huai River is 870 m^3.[12] Limited by geological and engineering technical conditions, the surface extraction of CBM mostly presents the states of low single well production (800−1500 m^3/day), fast attenuation speed, and inefficient development.[11] How to clarify the occurrence of CBM resources and strengthen the production of high-quality reserves have become urgent problems to be solved. Hence, it is necessary to investigate the origin, formation mechanism, and distribution characteristics of CBM in the Panxie Coal Mining Area.

The genetic types of CBM were divided into two types, namely, thermogenic gas and biogenic gas.[13−15] The former includes thermal degradation and pyrolysis gases, and the latter can be divided into primary and secondary biogenic gases. Various identification indicators were used for identifying the different genetic types of CBM. As for the CBM components,

Received: March 1, 2022
Accepted: May 11, 2022
Published: May 19, 2022

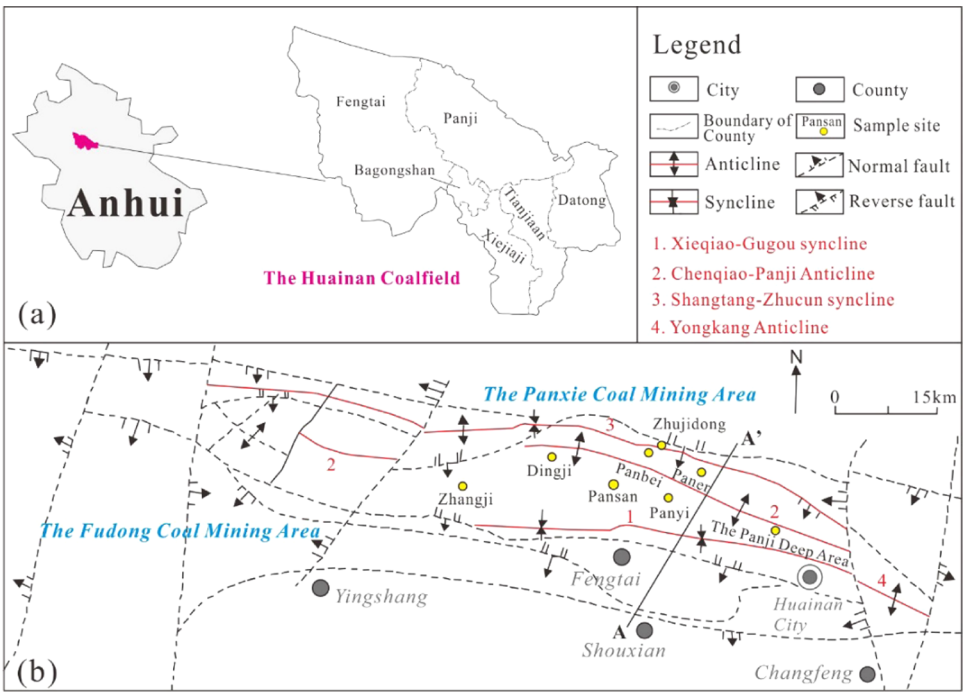

Figure 1. Location map (a) and the sample sites (b) from the Panxie Coal Mining Area in the Huainan Coalfield ((b) modified from ref 31).

such as the ratios of methane to the sum of ethane and propane ($C_1/(C_2 + C_3)$), the CDMI (CO_2−CH_4 index, 100% × $CO_2/(CO_2 + CH_4)$) was used,[16,17] for example, when the maximum vitrinite reflectance ($R_{o,max}$) value of CBM reservoirs is 0.70−1.00%, which is in the oil generation stage accompanied by wet gas. Generally, the concentrations of heavy hydrocarbon gases (C_{2+}), CO_2, and N_2 generated in CBM are relatively high. On the contrary, CBM exhibits the characteristics of dry gas. It may be biogenic gas or a mixture of biogenic and thermogenic gas, as this is a geochemical signature of biogenic gas and high-temperature pyrolysis gas.[18] In addition, the $C_1/(C_2 + C_3)$ value of thermogenic gas is <100, while that of biogenic gas is greater than 1000 and the value of mixed gas is 100−1000.[16]

The isotopic geochemical parameters, such as the carbon stable isotopes of alkane ($\delta^{13}C_{CH_4}$, $\delta^{13}C_{C_2H_6}$, and $\delta^{13}C_{C_3H_8}$) and CO_2 ($\delta^{13}C_{CO_2}$),[19,20] hydrogen stable isotopes (δD_{CH_4}),[21−23] and noble gas isotope ($^3He/^4He$),[22,24] were widely used to investigate the different genetic gases. For instance, $\delta^{13}C_{CH_4}$ = −55‰ is often used as the critical value for identifying biogenic and thermogenic gases.[25,26] When the value is <−55‰, it is biogenic gas; otherwise, it is thermogenic gas. Rice pointed out that the $\delta^{13}C_{CH_4}$ value of biogenic gas is in the range of −90 to −55‰, while that of thermogenic gas is >−55‰.[25] In addition, the associate plates with combined identification, including the plots of $C_1/(C_2 + C_3)$ versus $\delta^{13}C_{CH_4}$,[16,20] CDMI versus $\delta^{13}C_{CO_2}$,[27] $\delta^{13}C_{CH_4}$ versus $\delta^{13}D_{CH_4}$,[20,28] and $\delta^{13}C_{CH_4}$ versus $\delta^{13}C_{CO_2}$,[20] were usually considered as an intuitive and qualitative means to distinguish the genetic types of each component in CBM. For example, the plot of $C_1/(C_2 + C_3)$ versus $\delta^{13}C_{CH_4}$ can effectively distinguish thermogenic wet gas from biogenic dry gas. The quantitative identification methods based on the relationship between $\delta^{13}C_{CH_4}$ and $\delta^{13}C_{CO_2}$ and empirical equations were carried out for estimating the relative proportions of biogenic and thermogenic gases. Tao et al.[22] and Liu et al.[29] calculated the proportion of thermogenic methane in the Xinji Coalmine and around the Panji Mining Area of Huainan Coalfield on the basis of binary mixed mode; the percentage of thermogenic methane in the former region is 39.9%, while that of the latter region accounts for 80% of the total. Combined with the $R_{o,max}$ data, $\delta^{13}C_{CO_2}$, $\delta^{13}C_{CH_4}$, and empirical equations, Bao et al.[6] and Ayers[30] believed that the percentages of biogenic CBM samples are in the ranges of 47.65−51.21% and 15−30% for the Luling Mining Area of Huaibei Coalfield in China and the San Juan Basin in the United States, respectively.

Although geological conditions, geochemical characteristics, origins, and resource evaluation of CBM in the Panxie Coal Mining Area of Huainan Coalfield were reported by previous studies,[18,22,29,31] the genetic types, distribution characteristics, and accumulation models of CBM of different origins are still unclear, especially the lack of comprehensive research on CBM in different blocks and depths. With this focus, 16 CBM samples were collected from eight sites in the Panxie Coal Mining Area from a depth of 621−1494 m. Afterward, gas components and $\delta^{13}C_{CH_4}$, δD_{CH_4}, and $\delta^{13}C_{CO_2}$ were determined by experiments. Then, the genetic types of CBM and percentages of different genetic gases were analyzed. On the basis of analyses, the formation and evolution process and accumulation model of CBM were established. These results are beneficial to investigate the origin and accumulation mechanism and enrich the theoretical basis of CBM exploitation in the Panxie Coal Mining Area.[32]

2. GEOLOGICAL SETTING

The Panxie Coal Mining Area, located in the east part of Huainan Coalfield (Figure 1a), contains several coalmines such as Dingji Coalmine, Zhangji Coalmine, and Panyi Coalmine. The tectonic evolution process is mainly divided into three stages: continental period, continental margin period, and

https://doi.org/10.1021/acsomega.2c01227
ACS Omega 2022, 7, 17929−17940

Table 1. Components of CBM from the Panxie Coal Mining Area

sample sites	sample code	coal seam	buried depth (m)	$R_{o,max}$ (%)	composition (%)					C_1/C_{1-3} (%)	CDMI[a] (%)	$C_{1/2+3}$[b]
					CH_4	C_2H_6	C_3H_8	CO_2	N_2			
The Panji Deep Area	PD-1	13-1	1215	0.85	66.76	2.44	1.3	4.85	24.65	0.95	6.77	17.85
	PD-2	11-2	1281	0.80	79.73	3.19	0.8	1.3	14.98	0.95	1.60	19.98
	PD-3	3	1203	0.85	58.23	12.96	5.35	7.15	16.31	0.76	10.94	3.18
	PD-4	11-2	1438	0.82	88.86	5.41	0.59	5.06	0.08	0.94	5.39	14.81
	PD-5	8	1432	0.75	49.93	11.9	3.06	5.89	29.22	0.77	10.55	3.34
	PD-6	4-1	1494	0.79	84.92	5.41	1.43	4.84	3.4	0.93	5.39	12.42
Paner Coalmine	PE-1	1	518	0.72	68.14	3.37	1.42	8.32	18.75	0.93	10.88	14.23
Zhangji Coalmine	ZJ-1	11-2	648	0.73	80.36	4.81	1.06	4.14	9.63	0.93	4.90	13.69
	ZJ-2	6	546	0.72	95.42	1.27	0.36	0.74	2.21	0.98	0.77	58.54
Panyi Coalmine	PY-1	6	726	0.83	81.03	5.48	1.54	5.36	6.59	0.92	6.20	11.54
	PY-2	13-1	554	0.70	97.56	1.03	0.92	0.38	0.11	0.98	0.39	50.03
Pansan Coalmine	PS-1	8	621	0.73	94.63	0.26	0.13	4.66	0.32	1.00	4.69	242.64
Zhujidong Coalmine	ZJD-1	11-2	931	0.81	73.11	6.89	3.14	3.39	13.47	0.88	4.43	7.29
Dingji Coalmine	DJ-1	11-2	931	0.80	85.36	3.22	1.93	2.54	6.95	0.94	2.89	16.57
Panbei Coalmine	PB-1	4-1	754	0.78	90.04	1.08	1.19	6.16	1.53	0.98	6.40	39.67
	PB-2	4-1	760	0.79	94.26	0.42	1.37	2.14	1.81	0.98	2.22	52.66

[a]Note: C_1 = methane; C_2 = ethane; C_3 = propane; CDMI = 100% × $CO_2/(CO_2 + CH_4)$. [b]$C_{1/2+3} = C_1/(C_2 + C_3)$, that is, the ratio of C_1/C_{2+} concentrations. $R_{o,max}$ = the maximum vitrinite reflectance of coal samples.

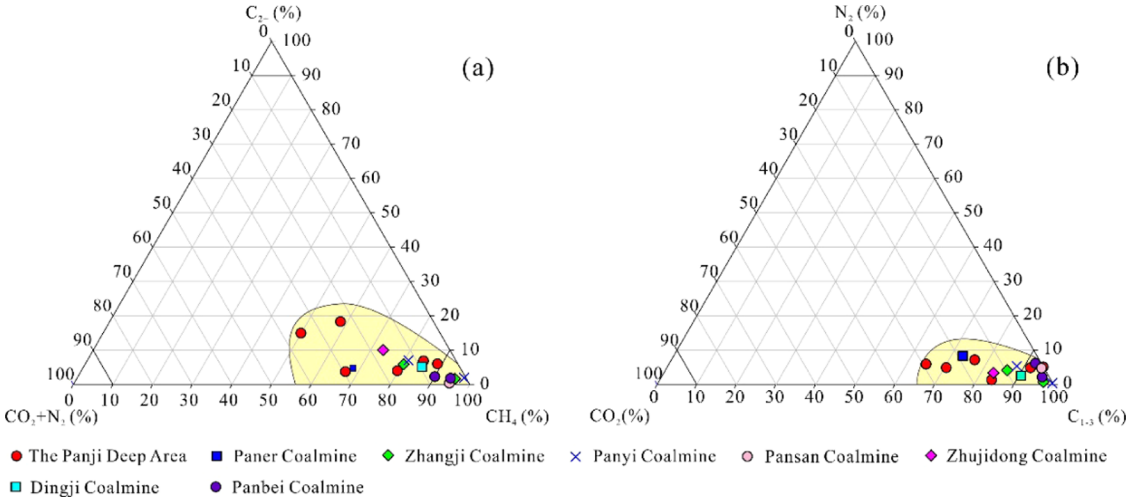

Figure 2. Plots of CH_4−C_{2+}−CO_2 + N_2 (a) and C_{1-3}−N_2−CO_2 (b).

intracontinental period. Subsequently, a synclinal structure with an axial near EW was formed (Figure 1b).[31,33] In addition, a series of anticlines and synclines from north to south are as follows: Shangtang-Zhucun syncline, Chenqiao-Panji anticline, Xieqiao-gugou syncline, and Yongkang anticline. The Upper Paleozoic Carboniferous−Permian source rocks are coal-bearing strata, including the Taiyuan, Shanxi, and Shihezi Formations. There are 19 mineable coal seams, which can be divided into seven coal-bearing sections from bottom to top. Among them, Nos. 7, 8, 11-2, and 13-1 coal seams are widely distributed and mineable in the whole area. The thermal evolution of CBM reservoirs from the Panxie Coal Mining Area, as shown in Table 1, is at the beginning of the thermogenic methane generation stage.

3. SAMPLES AND METHODS

On the basis of the aforementioned statement in Section 2, a total of 16 coal samples were collected from Nos.1, 3, 4-1, 6, 8, 11-2, and 13-1 coal seams in the selected coalmines of the Panxie Coal Mining Area, which is shown in Figure 1b and Table 1. The sampling method was in accordance with the China National Standard GB/T 29119−2012. The mass of each coal sample collected for CBM desorption was ∼200 to 300 g and then was quickly loaded into the canisters. To keep the composition of CBM unchanged, each canister was filled with coal samples, and the air was purged with argon before sampling. After the desorption experiment, CBM samples were gathered from a three-way valve on the pipelines with glass bottles.

The CBM components were determined using an HP6890 gas chromatograph (GC) in accordance with the China National Standard GB/T GB/T 13610-2014. Prior to the experiment, helium with a purity of 99.99% was used as the carrier gas to flush the channel at a flow rate of 5.4 mL/min. Afterward, the CBM sample was injected through the injection port, and then the chromatographic peaks were automatically recorded by the detector based on detection signals. Finally, the components were obtained through data processing. In the

https://doi.org/10.1021/acsomega.2c01227
ACS Omega 2022, 7, 17929−17940

experiment, the temperature of the GC oven was increased from 70 to 180 °C at a certain rate. After separation, the components were transported to the furnace for copper oxide activation treatment with a maximum temperature of 850 °C ($\delta^{13}C$ measurement) and 1400 °C (δD measurement), respectively. The values of $\delta^{13}C_{CH_4}$, δD_{CH_4}, and $\delta^{13}C_{CO_2}$ were calculated following the Vienna Pee Dee Belemnite standard, and the test accuracies were set to ±0.1, ±0.2, and ±1‰, respectively.

4. RESULTS

4.1. Component Characteristics of CBM. As shown in Table 1, the relative concentration of methane accounts for 49.93−95.42% (average, 80.52%), which indicates that methane is the main component of CBM in the Panxie Coal Mining Area. The concentration of ethane is between 0.26 and 12.96% (average, 4.32%), and samples with methane value >1% account for 87.50% of the total, and the main interval of numerical distribution is 2.44−6.89% (Figure 2). In addition, samples with ethane values >10% are distributed in the Panji Deep Area. Propane accounts for the smallest proportion of alkanes, which is 0.13−5.35% (average, 1.60%). The non-hydrocarbon gases mainly consist of N_2 and CO_2, with relative contents of 0.08−29.22% (average, 9.38%) and 0.38−8.32% (average, 4.18%), respectively. Moreover, CBM samples with N_2 value >10% are mainly concentrated in the Panji Deep Area, Paner Coalmine, and Zhujidong Coalmine. The dryness coefficient (C_1/C_{1-3}) and CDMI are 0.77−1.00 (average, 0.93) and 0.39−10.88% (average, 5.28%), respectively. The above results suggest that CBM samples are both dry and wet gases, and the proportion of the latter is 56.25%. Furthermore, the C_1/C_{2+3} value is in the range of 3.18−242.64 with an average of 36.15. As shown in Figure 3, the negative but

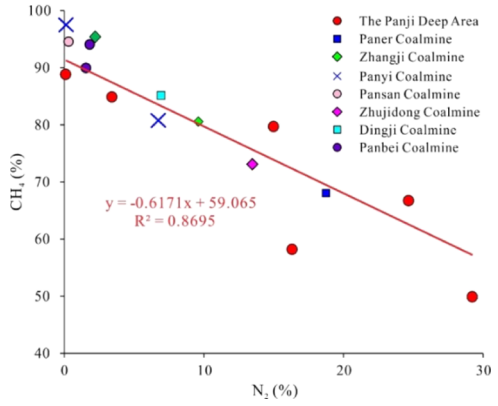

Figure 3. Correlation between N_2 and CH_4 concentrations of CBM samples.

significant linear relationship between N_2 and CH_4 concentrations refers to the infiltration of N_2 in the atmosphere during the formation or accumulation of CBM.[19]

4.2. Carbon and Hydrogen Stable Isotopes of the Selected Components in CBM. Table 2 lists the analytical data of the carbon and hydrogen stable isotopes of the selected components. The $\delta^{13}C_{CH4}$ values are distributed in the range of −65.44 to −32.38‰ with an average of −45.22‰. Among them, the highest value is in the Panji Deep Area, while the lowest value is in the Panyi Coalmine. Just from the perspective of numerical distribution, five anomalies from

Table 2. Stable Isotopes of CBM from the Panxie Coal Mining Area

sample sites	sample code	buried depth (m)	stable isotopes (‰)		
			$\delta^{13}C_{CH_4}$	δD_{CH_4}	$\delta^{13}C_{CO_2}$
The Panji Deep Area	PD-1	1215	−43.47	−164.15	−15.3
	PD-2	1281	−44.71	−181.24	−10.9
	PD-3	1203	−38.15	−173.47	−16.1
	PD-4	1438	−39.34	−189.63	−20.4
	PD-5	1432	−43.69	−176.96	−17.3
	PD-6	1494	−32.38	−155.34	−18.8
Paner Coalmine	PE-1	518	−33.47	−162.16	−14.2
Zhangji Coalmine	ZJ-1	648	−34.42	−156.82	−12.6
	ZJ-2	546	−61.10	−219.33	−10.1
Panyi Coalmine	PY-1	726	−33.20	−179.62	−18.5
	PY-2	554	−65.44	−213.61	−17.4
Pansan Coalmine	PS-1	621	−56.91	−226.84	−19.7
Zhujidong Coalmine	ZJD-1	931	−37.83	−191.06	−14.5
Dingji Coalmine	DJ-1	931	−39.64	−183.47	−19.3
Panbei Coalmine	PB-1	754	−57.45	−178.58	−10.4
	PB-2	760	−62.36	−174.64	−12.6

Zhangji, Panyi, Pansan, and Panbei Coalmines are below the lower limit ($\delta^{13}C_{CH_4}$ <−55‰) of biogenic gas, while others are greater than −55‰; this suggests that the selected CBM samples are both biogenic and thermogenic gases.[25,26] The δD_{CH_4} values are −226.84 to −156.82‰ with an average of −182.93‰, and the numerical distribution range of δD_{CH_4} is wider than that of $\delta^{13}C_{CH_4}$. In addition, the $\delta^{13}C_{CO_2}$ values are in the range of −19.7 to −10.1‰ with an average of −15.51‰.

5. DISCUSSION

5.1. Genetic Types of CBM. For ease of comparison among CBM samples from the Panxie Coal Mining Area, the plots of correlation between buried depth and components were established and are shown in Figure 4. Figure 4a shows that the methane concentration of almost all of the CBM samples from a burial depth of <800 m is more than 80%, and the detected alkanes have similar distribution characteristics (Figure 4b). It is worth noting that the relative concentrations of methane and alkanes of CBM samples from the Panji Deep Area and Zhujidong Coalmine have relatively low values, and most of them are distributed in the ranges of <80 and <90%, respectively. On the whole, there are weak and negative correlations between the above alkanes and burial depth. On the contrary, the C_{2+} concentration has a weak but positive correlation with burial depth (Figure 4c).

As shown in Figure 4d, CBM samples from a burial depth of >800 m show the characteristics of dry gases, while samples with a relatively shallow burial depth are mostly wet gases. Based on the maturity ($R_{o,max}$ = 0.81−1.09%) of coals from the Huainan Coalfield[18,22,29,34] and theory by Scott et al.,[14] coals in the Panxie Coal Mining Area have not yet reached the overmature stage of generating high-temperature pyrolysis gas.[18] Therefore, in terms of components of CBM and maturity of coals, there may be secondary biogenic gases. Figure 4e,f shows that CO_2 and N_2 concentrations of a considerable number of CBM samples from a burial depth of

https://doi.org/10.1021/acsomega.2c01227
ACS Omega 2022, 7, 17929−17940

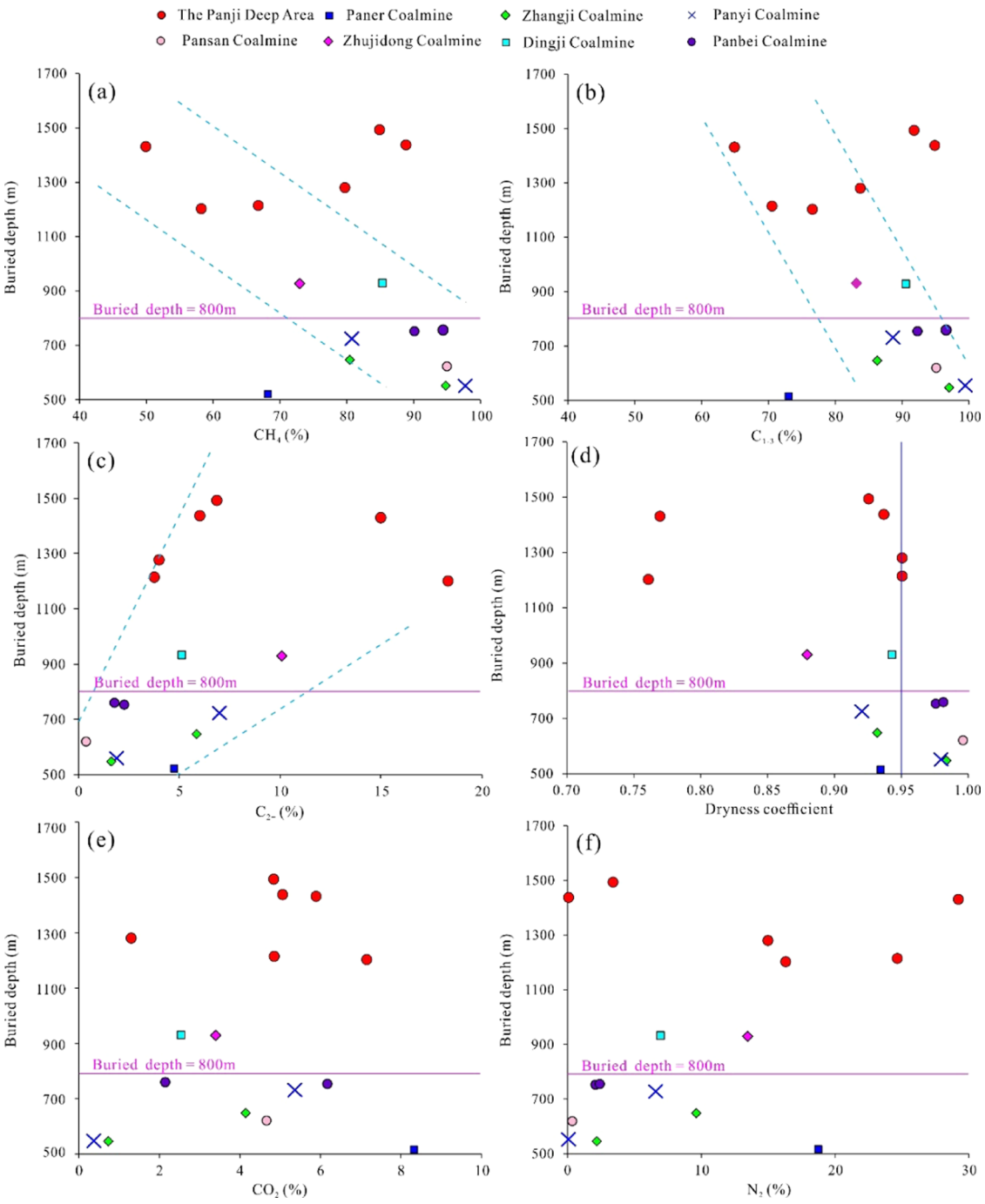

Figure 4. Relationships between buried depth and alkanes (a−c), dryness coefficient (d), CO_2 (e), and N_2 (f) of the selected CBM samples.

<800 m exhibit values of <5 and <10%, respectively, which are significantly different from the deeper buried samples.

In addition, the relationships between the burial depth and $\delta^{13}C_{CH_4}$ and δD_{CH_4} of CBM samples were analyzed, as shown in Figure 5. On the whole, the $\delta^{13}C_{CH_4}$ is complex, and CBM reservoirs with a similar maturity exhibit large variation values. As shown in Figure 5a, $\delta^{13}C_{CH_4}$ of CBM samples from a buried depth of >800 m exhibits higher values than those from a buried depth of <800 m with five exceptions from Panbei, Pansan, Zhangji, and Panyi Coalmines. Of note, a similar phenomenon is shown in δD_{CH_4} values (Figure 5b). On the whole, the $\delta^{13}C_{CH_4}$ value increases as the burial depth increases. Dai et al.[35] believed that most of the relevant laws of CBM in coalmine and primary CBM in reservoirs were inconsistent, that is, the value of $\delta^{13}C_{CH_4}$ in shallow coalbeds decreased, while that of medium and deep wells was basically the same. Therefore, obvious secondary changes occurred in CBM from the Panxie Coal Mining Area. According to the research results from Smith and Pallasser,[26] the value is −60 to −50‰; the $\delta^{13}C_{CH_4}$ of secondary biogenic gas in the Upper Silesian Basin is −79.9 to −44.5‰. Obviously, the abnormal samples from Zhangji, Panyi, Pansan, and Panbei Coalmines are in the range of the biogenic region, but toward the heavier end, it is considered the result of a mixture of biogenic and thermogenic gases. Li et al.[15] considered that $\delta^{13}C_{CH_4}$ values of

https://doi.org/10.1021/acsomega.2c01227
ACS Omega 2022, 7, 17929−17940

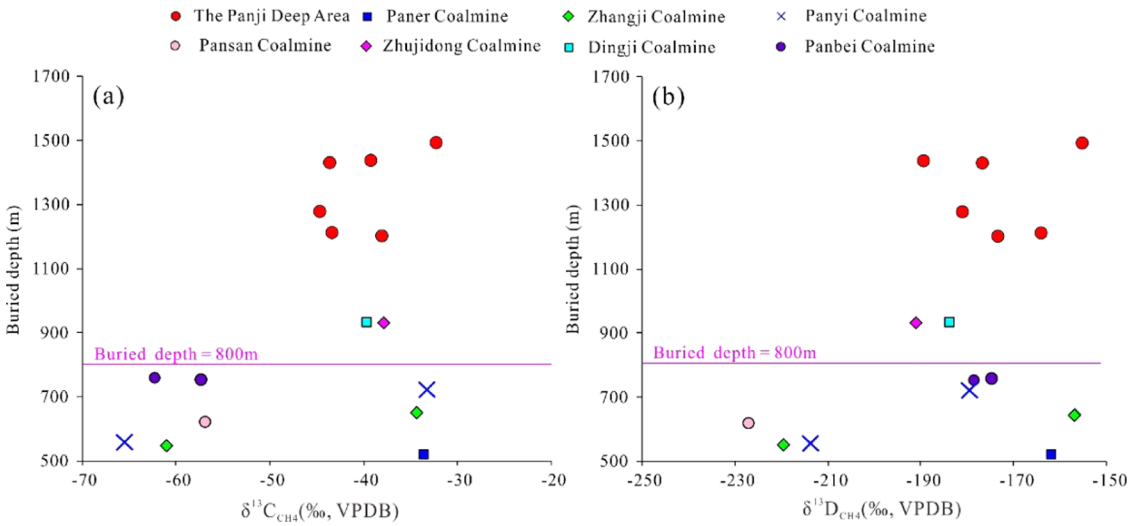

Figure 5. Correlations between buried depth and $\delta^{13}C_{CH_4}$ (a) and δD_{CH_4} (b) of CBM samples.

CBM samples from Hancheng, Liulin, Baode, and Xingxian blocks of the Ordos Basin are linearly and positively correlated with burial depth, and the samples of the latter two blocks can be classified as original and desorption belts based on the linear correlation. This division result is controlled by the stable environment of gas generation and evolution. Based on the analysis results of coal reservoirs with similar maturity ($R_{o,max}$ = 0.65−0.90%), Qin et al.[36] compared the relationship between $\delta^{13}C_{CH_4}$ and burial depth in multiple coalfields of North China and pointed out that $\delta^{13}C_{CH_4}$ becomes higher with increasing burial depth. In addition, the increase rate of $\delta^{13}C_{CH_4}$ shows turning points at −1000, −1500, and −2000 m, which correspond to desorption, transition, and primary zones, respectively. The boundaries among the above zones vary in different regions and are related to the lower limit depth of weathering belt and coal rank.

As mentioned in analyses, the $R_{o,max}$ of coal seams corresponding to the selected CBM samples is in the range of 0.70−0.85% and is at the beginning of the thermogenic methane generation stage. The variations in $\delta^{13}C_{CH_4}$ and δD_{CH_4} values may be related to the fractionation effect of the thermal evolution of coals, the effect of isotopic fractionation in the process of desorption, diffusion, and seepage of CBM, and the effects of hydrogeological conditions and secondary biogenic gases.[15,21,28,37,36]

As confirmed by previous scholars, multiple indexes were used to evaluate the genetic types of CBM by the differences in stable isotopes and compositions, which provides a means to distinguish the overlapped zones of CBM with different origins, instead of using a single index.[7,28,35,38] Based on the plot of C_1/C_{2+3} versus $\delta^{13}C_{CH_4}$, shown in Figure 6, the thermogenic gas is the primary type, while microbial activity has a significant impact on five CBM samples and led to lower $\delta^{13}C_{CH_4}$ values of CBM samples in the mixing region. Figure 7 shows the data of $\delta^{13}C_{CH_4}$ and δD_{CH_4}, the distribution of all points illustrates that CBM samples have multiple origins. Similar to Figure 6, five CBM samples fall into the microbial region with CO_2 reduction and mixing areas of thermogenic and biogenic, and others are distributed in the region for the thermogenic process. As shown in Figure 8, all data points fall

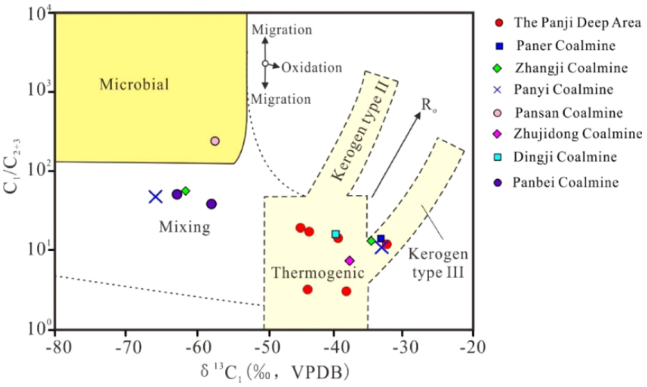

Figure 6. Genetic characterization of CBM from the Panxie Coal Mining Area (the plate modified from ref 20).

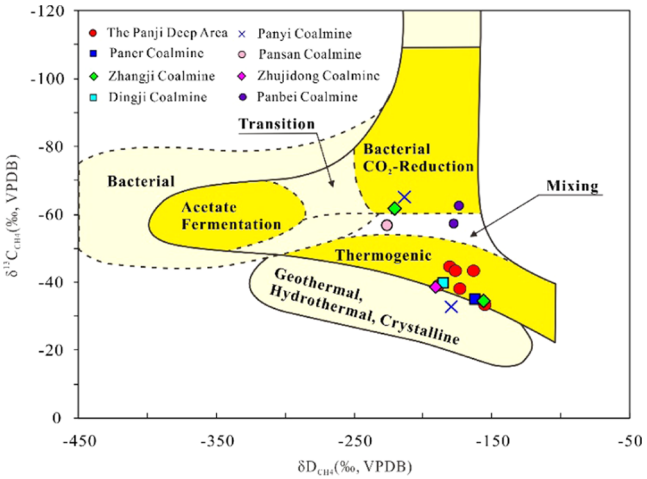

Figure 7. Genetic characterization of CBM based on the plot of $\delta^{13}C_{CH_4}$ and δD_{CH_4} (the plate modified from ref 19).

into the "Coal and/or type III kerogen decarboxylation (thermogenic CO_2)" region, which implies the thermogenic origin of CO_2. Figure 9 shows the carbon stable isotope fractionation of CH_4 and CO_2, and most of the CBM samples are located in the thermogenic region; other samples from Panyi, Panbei, and Zhangji Coalmines are mixed origin gases,

https://doi.org/10.1021/acsomega.2c01227
ACS Omega 2022, 7, 17929−17940

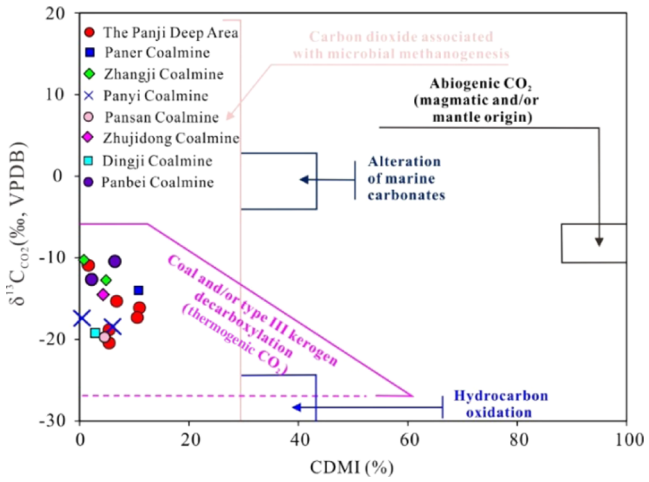

Figure 8. Genetic characterization of CO_2 in CBM from the Panxie Coal Mining Area (the plate modified from ref 27).

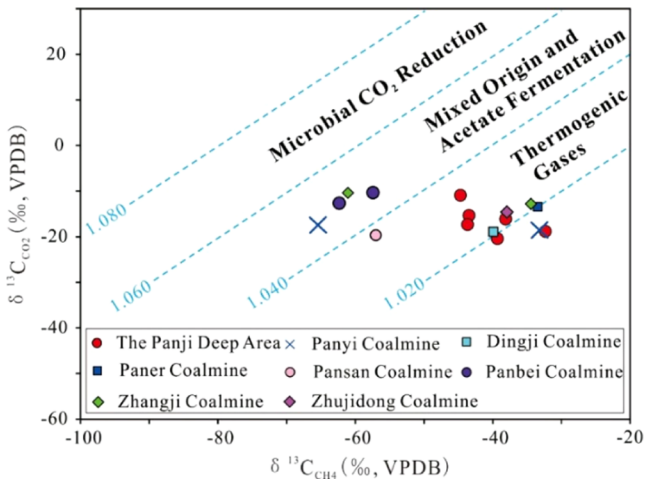

Figure 9. Stable isotopes of CH_4 and CO_2 of CBM from the Panxie Coal Mining Area (the plate modified from ref 20).

which is consistent with the results in Figure 6. Obviously, although the microbial activity is strong, thermogenic gas is still well preserved.

The above analyses definitely show that in addition to the exceptions from Panbei, Pansan, Zhangji, and Panyi Coalmines, values of $\delta^{13}C_{CH_4}$ and δD_{CH_4} from other sample points of the Panxie Coal Mining Area are characterized by thermogenic gases with $\delta^{13}C_{CH_4}$ higher than −44.71‰ and δD_{CH_4} greater than −191.06‰. For the five exception samples, the values of $\delta^{13}C_{CH_4}$ and δD_{CH_4} are <−55 and −226.84 to −174.64‰, respectively, which are characterized by mixed gases of biogenic and thermogenic gases. Similarly, the CH_4 concentration of the above five CBM samples is in the range of 90.04−97.56%, and the dryness coefficient is 0.98−1.00. Comparably, the values of other samples are 49.93−88.86% and 0.76−0.95. The thermal evolution of CBM reservoirs from the Panxie Coal Mining Area, as shown in Table 1, is at the beginning of the thermogenic methane generation stage. Therefore, the CBM samples are not of primary biogenic gases but secondary biogenic gases. Hence, the CBM samples are mainly thermogenic gases, and the biogenic gases are confirmed by following the values of component concentration, dryness coefficient, and stable isotope.

5.2. Percentage of Different Genetic CBMs. The $\delta^{13}C_{CH_4}$ values vary significantly worldwide. Tao et al.[22] summarized that the main interval value for biogenic gases is −75 to −70‰ according to the $\delta^{13}C_{CH_4}$ values worldwide, but the lowest value of which is −72.27‰ in the ever reported studies of Huainan Coalfield. Li et al.[37] believed that −75.5‰ is the end member of the $\delta^{13}C_{CH_4}$ value in the Huaibei Coalfield, but the lowest value is −87.2‰ for the biogenic CBM in the Dafosi minefield of the Ordos Basin.[7] Therefore, −75.5‰ is chosen as the end value of biogenic CBM even if the minimum value has not been tested. Based on the above analyses from Section 5.1, both thermogenic and biogenic gases exist in the Panxie Coal Mining Area, and the relative percentages of different origins can be considered as[38]

$$aA + bB = C \quad (1)$$

$$a + b = 1 \quad (2)$$

where a is the percentage of thermogenic gas (%), b is the percentage of biogenic gas (%), A is the $\delta^{13}C_{CH_4}$ value of thermogenic gas (‰), B is the end value of $\delta^{13}C_{CH_4}$ for biogenic gas, that is, −75.5‰, and C is the tested $\delta^{13}C_{CH_4}$ value, as shown in Table 2. In addition, A can be represented as[38]

$$A = -26.20 \log R_{o,\max} - 34.12 \quad (R_{o,\max} < 1.30\%) \quad (3)$$

$$A = 25.85 \log R_{o,\max} - 43.08 \quad (R_{o,\max} \geq 1.30\%) \quad (4)$$

Based on the above equations, the percentage of thermogenic gas is 70.11−97.86%, whereas that of biogenic gas is 58.65−77.86% for five samples from Zhangji, Panyi, Pansan, and Panbei Coalmines. This result suggests that the CBM samples of Panxie Coal Mining are mainly thermogenic gases, followed by biogenic gases (Table 3).

Table 3. Percentages of Different Genetic CBMs in the Panxie Coal Mining Area

sample sites	sample code	C (‰)	B (‰)	A (‰)	a (%)	b (%)
The Panji Deep Area	PD-1	−43.47	−75.5	−32.27	74.09	25.91
	PD-2	−44.71	−75.5	−31.58	70.11	29.89
	PD-3	−38.15	−75.5	−32.27	86.40	13.60
	PD-4	−39.34	−75.5	−31.86	82.86	17.14
	PD-5	−43.69	−75.5	−30.85	71.24	28.76
	PD-6	−32.38	−75.5	−31.44	97.86	2.14
Paner Coalmine	PE-1	−33.47	−75.5	−30.38	93.16	6.84
Zhangji Coalmine	ZJ-1	−34.39	−75.5	−30.54	91.43	8.57
	ZJ-2	−61.1	−75.5	−30.38	31.92	68.08
Panyi Coalmine	PY-1	−33.2	−75.5	−32.00	97.24	2.76
	PY-2	−65.44	−75.5	−30.06	22.14	77.86
Pansan Coalmine	PS-1	−56.91	−75.5	−30.54	41.35	58.65
Zhujidong Coalmine	ZJD-1	−37.83	−75.5	−31.72	86.05	13.95
Dingji Coalmine	DJ-1	−39.64	−75.5	−31.58	81.65	18.35
Panbei Coalmine	PB-1	−57.45	−75.5	−31.29	40.83	59.17
	PB-2	−62.36	−75.5	−31.44	29.82	70.18

https://doi.org/10.1021/acsomega.2c01227
ACS Omega 2022, 7, 17929−17940

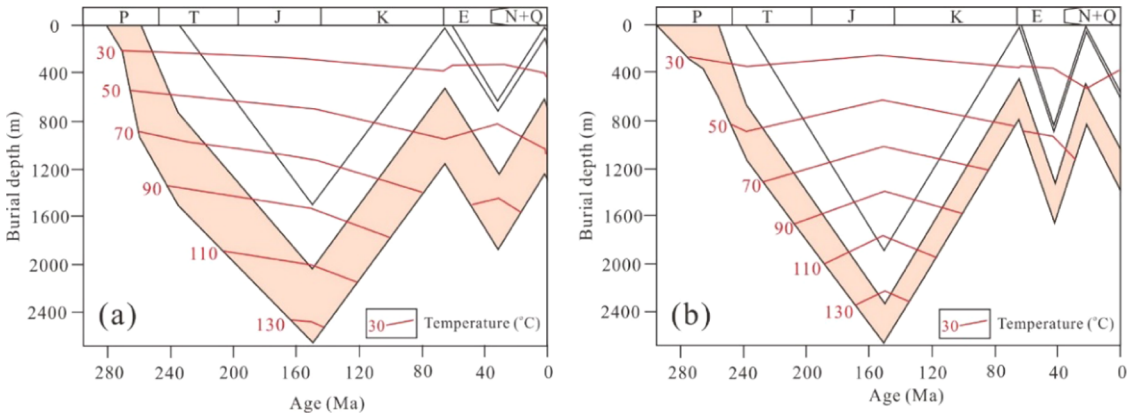

Figure 10. Geological evolution histories of Permian coal-bearing strata at positions of the Panji Deep Area (a) and Dingji Coalmine (b).

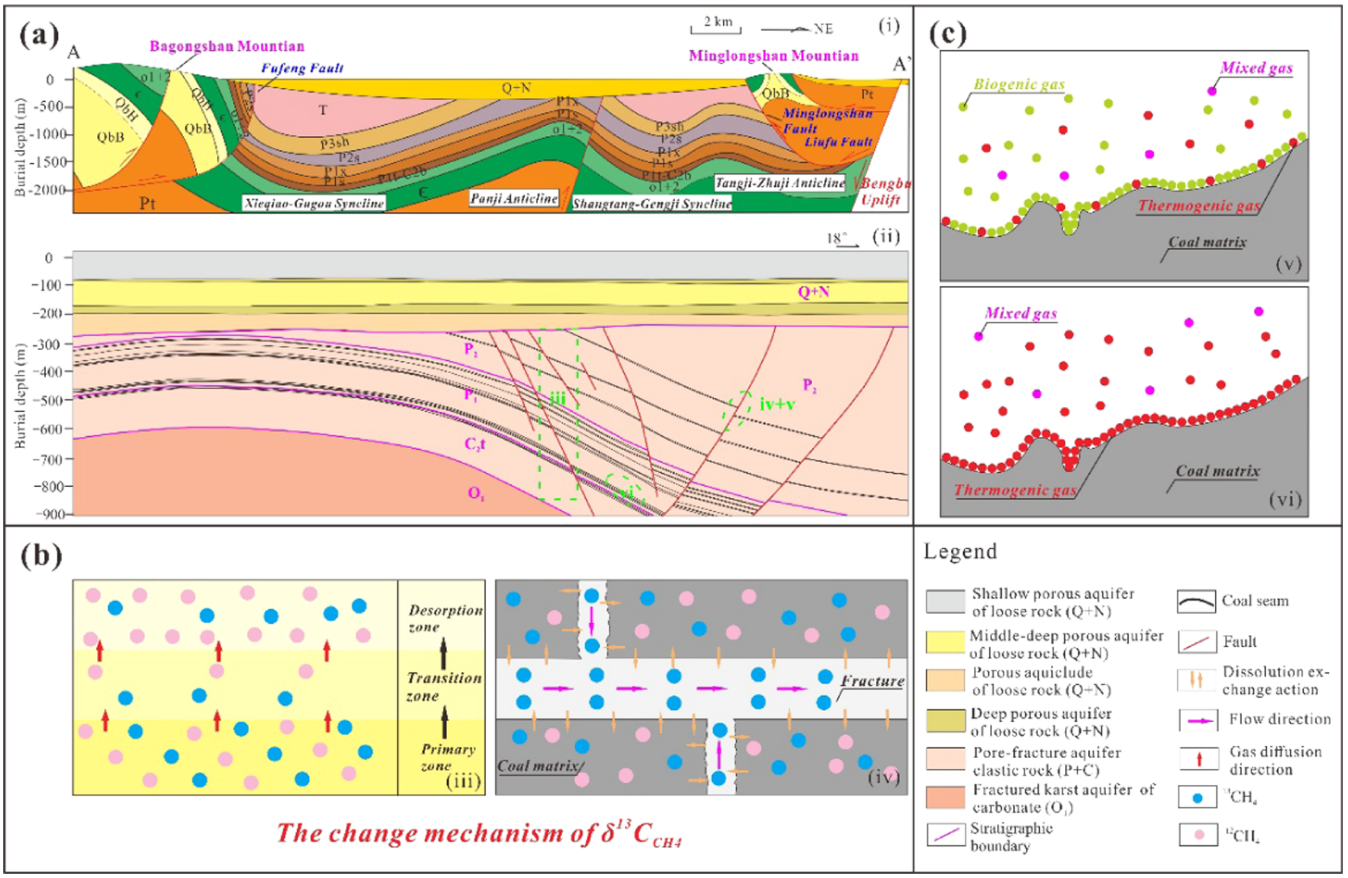

Figure 11. Change mechanism of $\delta^{13}C_{CH_4}$ and accumulation model of CBM from the Panxie Coal Mining Area. Note: (a) Structural profile of the Panxie Coal Mining Area (i) and Pansan Coalmine (ii); (b) the change mechanism of $\delta^{13}C_{CH_4}$ (iii, iv); (c) CBM accumulation model (v, vi) (modified by refs 31, 43).

Generally, biogenic gas can be produced in two ways, namely, CO_2 reduction and acetic acid fermentation. The δD_{CH4} value of the former is −250 to −150‰, and that of the latter is −400 to −250‰. Of note, the hydrogen atoms of methane are all derived from water, and the changes in the δD_{CH_4} value of the above two mechanisms can be expressed by eqs 5 and 6[25]

$$\delta D_{CH_4} = \delta D_{H_2O} - 160 \pm 10‰ \quad (5)$$

$$\delta D_{CH_4} = 0.14 \times \delta D_{H_2O} - 384‰ \quad (6)$$

In the Panxie Coal Mining Area, the δD_{CH_4} value of limestone karstic water of the Taiyuan Formation is −81.37 to −30.87‰ with an average of −58‰.[39] Due to the separation of mud rocks among coal measure aquifers, there is no close hydraulic connection under the undisturbed state. However, the hydraulic head pressure of the limestone karstic of the Taiyuan Formation exceeds the maximum allowable water pressure of the rock stratum at the bottom of the coal measures. Therefore, the water in the limestone aquifer of the Taiyuan Formation may directly come from the bottom of coal measures.[40] On the basis of the above analysis, the δD_{CH_4} value

https://doi.org/10.1021/acsomega.2c01227
ACS Omega 2022, 7, 17929−17940

may have a similar distribution interval to that of limestone karstic water of the Taiyuan Formation. Then, substituting the above numerical value of −81.37 to −30.87‰ into eq 5, the calculated δD_{CH_4} value is −241.37 ± 10 to −190.87 ± 10‰. By comparison, the δD_{CH_4} value for the above five samples ranges from −226.84% to −174.64‰, all of the values are close to the calculated values by eq 5. The analysis result shows that if there is a certain amount of biogenic gases in CBM samples, it is more likely to be secondary biogenic gases generated by CO_2 reduction.

5.3. CBM Formation and Evolution Process. The geological evolution histories of the Permian coal-bearing stratum have been simulated by previous scholars.[18,31,41,42] Based on the data of $R_{o,max}$, strata, and geological age of related boreholes from the Panji Deep Area and Dingji Coalfield, the thermal evolution process of coal seams was revealed by Thermodel for Windows 2008 software. As shown in Figure 10 and the related results, the process can be divided into the following stages: (1) Humid gas generation stage (about 290−150 Ma): In the early stage, there was a time when the paleogeotherm was <60 °C from the beginning of the rapid decline of the Permian to the middle of early Permian−early Jurassic, and different strata of Permian may have a long period of biogenic gas generation.[18] In the middle and late stages, the Permian was deeply buried (exceeding 2400 m), and the coal measures were in the stage of thermal catalytic petroleum and humid gas was the main product.[29] (2) Stage of structural destruction of CBM reservoirs during the late Jurassic−Cretaceous (about 140−65 Ma): Although thermogenic gas and biogenic gas were generated in this stage, the CBM was desorbed and diffused due to the structural uplift. Notably, coal seams in the Panji and Dingji regions superimposed magmatic metamorphism on the basis of regional metamorphism. However, limited by the scale, heat, and depth of magmatic activity from late Jurassic to early Cretaceous, the influence range of the superimposed gas generation process is limited.[18] The coalification degree of Permian coals in Huainan Coalfield was completed at 120 Ma. Thus, the generation process of thermogenic gas from coal has been completely terminated. (3) The generation stage of thermogenic and biogenic gases in local horizons during the early−middle Paleogene (65−23 Ma): Due to the subsidence, the paleogeotherm of coal seams in the lower Permian exceeded 60 °C, and thermogenic gas was mainly generated. By contrast, the paleogeotherm of coal seams in the upper Permian was <60 °C, and there was a possibility of secondary biogenic gas. (4) The re-destruction stage of tectonic uplift from the end of Paleogene to the present (23−0 Ma). In this stage, even if CBM was generated, desorption-diffusion fractionation occurred due to structural uplift.

Figure 11 shows the change mechanism of $\delta^{13}C_{CH_4}$ and the accumulation model of CBM from the Panxie Coal Mining Area. As shown in Figure 11a, under the transformations of Indosinian, Yanshan, and Himalayan movements, the structural pattern of the Shangyao-Minglongshan thrust structural belt on the north side, and Fufeng thrust nappe structural belt on the south side and Huainan Syncline in the middle was formed. In addition, the differences exist in vertical distributions of main aquifers, coal seams, and faults in the structural profile of Paner Coalfield. With this focus, the $\delta^{13}C_{CH4}$ value varies with burial depth. In general, it can be divided into three parts: primary zone, transition zone, and desorption zone.[43] The CBM generated by the coal seam itself in the "desorption zone" has been lost under the influence of internal and external factors. At present, most of the CBM existing in the zone is the result of gradual diffusion and migration of CBM generated by the "primary zone" after long-term desorption (Figure 11b). From the molecular point of view, due to the difference in isotopic polarity of methane molecules, the desorption order of $^{12}CH_4$ is preferred over that of $^{13}CH_4$, and then $\delta^{13}C_{CH4}$ fractionation occurs in coal seams.[6,36] As a result, $^{12}CH_4$ methane is relatively enriched, which shows that the $\delta^{13}C_{CH4}$ value decreases the diffusion−migration process, thus resulting in a vertical zoning sequence that varies with burial depth. In addition, due to the differences in the analytical diffusion properties of different components and carbon isotopes, CBM in the desorption zone is rich in light methane and has a small value of $\delta^{13}C_{CH_4}$. The desorption-diffusion fractionation of CBM is a kind of vertical diffusion fractionation, which causes the $\delta^{13}C_{CH_4}$ value of the shallower coal seam to be lower than that of the deeper coal seam (Figure 5a). Therefore, desorption-diffusion fractionation mainly occurs in areas with multiple coal seams, structural uplift, and deeper coal seams with higher $\delta^{13}C_{CH_4}$ values, the detailed evidence is shown in Table 2 and Figure 11a (the position of iii).

As shown in Figure 11a, the Panxie Coal Mining Area was covered with a huge Cenozoic loose layer and was cut by thrust faults and oblique faults on the north and south wings, forming a relatively closed hydrogeological unit.[39] The main water sources of the Panxie Coal Mining Area are the limestone water from Ordovician and the Carboniferous Taiyuan Formation.[44] Based on the analyses of the sedimentary system and the unconformity interface in tectonic evolution stages, Zhang et al. believed that several groundwater dynamic mechanisms have occurred during geological periods in the Huainan Coalfield,[28] which led to the reduction of gas content of coal seam.[45] In addition, the effect of groundwater dissolution on $\delta^{13}C_{CH_4}$ cannot be ignored. The flowing groundwater is more likely to dissolve $^{13}CH_4$ and take it away from the coal seam; thus, the $\delta^{13}C_{CH_4}$ value is generally lower.[28,46] Liu et al.[29] believed that there are individual abnormal values in $\delta^{13}C_{CH_4}$of CBM in the Panji Mining Area, and hydrodynamic conditions account for the largest proportion of all factors. CBM samples close to the aquifer of the Taiyuan Formation have a relatively lower $\delta^{13}C_{CH_4}$ value, which further confirms the influence of the dissolution fractionation effect on the $\delta^{13}C_{CH_4}$ value. As demonstrated in a previous study,[11] the groundwater of the Panji Deep Area is generally in a stagnant state due to the bedrock aquifer cutting off the water supply of bare areas. The groundwater from Ordovician has a closely hydraulic connection with the Carboniferous Taiyuan Formation in Zhangji, Panyi, and Paner Coalmines.[39,44] With this focus, the $\delta^{13}C_{CH_4}$ values vary in different regions.

The dissolution of groundwater is similar to dissolution fractionation, but this phenomenon mainly occurs in the runoff zone of groundwater. Generally, CBM samples with similar components but heavier isotope values are relatively stable and are hard to dissolve after dissolving into formation water. As water moves into the next set of formations, heavier isotopic gases are gradually enriched to form gas isotopic fractionation. Hence, when the groundwater runoff condition is strong, the

https://doi.org/10.1021/acsomega.2c01227
ACS Omega 2022, 7, 17929−17940

reason for a lower $\delta^{13}C_{CH_4}$ value of CBM is mostly the dissolution of flowing groundwater.[28] In addition, as a channel between shallow porous aquifers of loose layer and coal measures, the fault brings surface water and methanogens into coal seams to a certain extent. Because of the downward migration of water, external fungi and surface water are brought into coal seams, thus generating secondary biological CBM dominated by CH_4 and CO_2 (the position of iv and v in Figure 11a). Figure 11c shows the mixture of secondary biogenic and thermogenic gases under certain conditions. As a result, this mixing effect leads to a lower $\delta^{13}C_{CH_4}$ value and a lower C_{2+} concentration of CBM, which can simultaneously explain the phenomenon of "drying and lighting" of CBM (Tables 1 and 2). To sum up, accumulation models of different genetic types of CBM from the Panxie Coal Mining Area are correlated with the burial depth of coal seams, location, and types of faults and aquifers.

6. CONCLUSIONS

Based on the measurements of components, $\delta^{13}C_{CH_4}$, δD_{CH_4}, and $\delta^{13}C_{CO_2}$ of CBM samples from the Panxie Coal Mining Area of Huainan Coalfield, the genetic types, the proportions of different genetic gases, and the accumulation model of CBM were analyzed. The conclusions are drawn as follows:

(1) CBM samples of the Panxie Coal Mining Area are dominated by methane, and the concentrations are mainly distributed in the range of 73.11−95.42%. The dryness coefficient is 0.77−1.00 (average, 0.93), which suggests that CBM samples are both dry and wet gases. In addition, the C_1/C_{2+3} value is 3.18−242.64, with a mean value of 36.15.

(2) The $\delta^{13}C_{CH4}$ values are distributed in the range of −65.44 to −32.38‰ (average, −45.22‰), basically within the range of thermogenic gases and five anomalies in the region of biogenic gases. The δD_{CH4} values are −226.84 to −156.82‰ (average, −182.93‰), and the $\delta^{13}C_{CO_2}$ values are −19.7 to −10.1‰ (average, −15.51‰). The genetic type of CBM samples is predominately by thermogenic gases, followed by secondary biogenic gases with CO_2 reduction.

(3) Desorption-diffusion fractionation and the effect of groundwater dissolution mainly occur in areas with multiple coal seams, structural uplift, and deeper coal seams with higher $\delta^{13}C_{CH_4}$ values. In addition, the downward migration of water, external fungi, and surface water are brought into coal seams, thus generating secondary biological CBM dominated by CH_4 and CO_2. Accumulation models of different genetic types of CBM are correlated related to the burial depth of coal seams, location, and type of faults and aquifers.

AUTHOR INFORMATION

Corresponding Authors

Qiang Wei − *School of Resources and Civil Engineering, Suzhou University, Suzhou 234000, P. R. China; Institute of Energy, Hefei Comprehensive National Science Center, Hefei 230031, P. R. China; National Engineering Research Center of Coal Mine Water Hazard Controlling, Anhui 234000, P. R. China;* orcid.org/0000-0001-8068-1253; Email: 1404579796@qq.com

Baolin Hu − *School of Earth and Environment, Anhui University of Science and Technology, Huainan 232001, P. R. China*; Email: Baolinhu@sina.com

Huihuang Fang − *Institute of Energy, Hefei Comprehensive National Science Center, Hefei 230031, P. R. China; School of Earth and Environment, Anhui University of Science and Technology, Huainan 232001, P. R. China*; Email: huihuangfang@aust.edu.cn

Authors

Song Chen − *School of Resources and Civil Engineering, Suzhou University, Suzhou 234000, P. R. China; National Engineering Research Center of Coal Mine Water Hazard Controlling, Anhui 234000, P. R. China*

Songbao Feng − *School of Resources and Civil Engineering, Suzhou University, Suzhou 234000, P. R. China; National Engineering Research Center of Coal Mine Water Hazard Controlling, Anhui 234000, P. R. China*

Cancan Wu − *School of Resources and Civil Engineering, Suzhou University, Suzhou 234000, P. R. China; National Engineering Research Center of Coal Mine Water Hazard Controlling, Anhui 234000, P. R. China*

Chunshan Zheng − *Institute of Energy, Hefei Comprehensive National Science Center, Hefei 230031, P. R. China*

Complete contact information is available at: https://pubs.acs.org/10.1021/acsomega.2c01227

Author Contributions

The manuscript was written with contributions from all authors, and all authors have approved the final version of the manuscript.

Notes

The authors declare no competing financial interest.

ACKNOWLEDGMENTS

This work was financially supported by the University Synergy Innovation Program of Anhui Province (No. GXXT-2021-018), the University Natural Science Research Project of Anhui Province (No. KJ2021A1113), the Start-up Fund for Doctoral Research of Suzhou University (No. 2019jb20), the Green Mine Research Center of Suzhou University (No. 2021XJPT53), the investigation on the national conditions of identified mineral resources in Anhui Province (No. 2021xhx155), and horizontal project of Suzhou University (No. 2021xhx034). The authors express their gratitude to the editors and reviewers for their valuable comments on the paper.

REFERENCES

(1) Li, Y.; Wang, Z. S.; Tang, S. H.; Elsworth, D. Re-evaluating adsorbed and free methane content in coal and its ad- and desorption processes analysis. *Chem. Eng. J.* **2022**, *428*, No. 131946.

(2) Li, Y.; Wang, Y. B.; Wang, J.; Pan, Z. J. Variation in permeability during CO_2−CH_4 displacement in coal seams: Part1 − Experimental insights. *Fuel* **2020**, *263*, No. 116666.

(3) Liu, C. L.; Zhu, J.; Che, C. B.; Yang, H. L.; Fan, M. Z. Methodologies and results of the latest assessment of coalbed methane resources in China. *Nat. Gas Ind.* **2009**, *29*, 130−132.

(4) Li, H. Y.; Lau, H. C.; Huang, S. China's coalbed methane development: A review of the challenges and opportunities in subsurface and surface engineering. *J. Pet. Sci. Eng.* **2018**, *166*, 621−635.

(5) Chen, B.; Stuart, F. M.; Xu, S.; Györe, D.; Liu, C. Evolution of coal-bed methane in Southeast Qinshui Basin, China: Insights from stable and noble gas isotopes. *Chem. Geol.* **2019**, *529*, No. 119298.
(6) Bao, Y.; Wei, C.; Neupane, B. Generation and accumulation characteristics of mixed coalbed methane controlled by tectonic evolution in Liulin CBM field, eastern Ordos Basin, China. *J. Nat. Gas Sci. Eng.* **2016**, *28*, 262−270.
(7) Bao, Y.; Wang, W. B.; Ma, D. M.; Shi, Q. M.; Ali, A.; Lv, D. K.; Zhang, C. K. Gas Origin and Constraint of $\delta^{13}C(CH_4)$ Distribution in the Dafosi Mine Field in the Southern Margin of the Ordos Basin, China. *Energy Fuels* **2020**, *34*, 14065−14073.
(8) Li, Y.; Zhang, C.; Tang, D. Z.; Gan, Q.; Niu, X. L.; Wang, K.; Shen, R. Y. Coal pore size distributions controlled by the coalification process: An experimental study of coals from the Junggar Ordos and Qinshui basins in China. *Fuel* **2017**, *206*, 352−363.
(9) Wei, Q.; Li, X. Q.; Hu, B. L.; Zhang, X. Q.; Zhang, J. Z.; He, Y. K.; Zhang, Y. C.; Zhu, W. W. Reservoir characteristics and coalbed methane resource evaluation of deep-buried coals: A case study of the No.13-1 coal seam from the Panji Deep Area in Huainan Coalfield, Southern North China. *J. Pet. Sci. Eng.* **2019**, *179*, 867−884.
(10) Wei, Q.; Zheng, K. G.; Hu, B. L.; Li, X. Q.; Feng, S. B.; Jiang, W.; Zhu, W. W.; Feng, W. Q. Methane Adsorption Capacity of Deep-Buried Coals Based on Pore Structure in the Panji Deep Area of Huainan Coalfield, China. *Energy Fuels* **2021**, *35*, 4775−4790.
(11) Wei, Q.; Hu, B. L.; Li, X. Q.; Feng, S. B.; Xu, H. J.; Zheng, K. G.; Liu, H. H. Implications of geological conditions on gas content and geochemistry of deep coalbed methane reservoirs from the Panji Deep Area in the Huainan Coalfield, China. *J. Nat. Gas Sci. Eng.* **2021**, *85*, No. 103712.
(12) Zhang, W. Y.; Dou, X. Z.; Liu, G. J.; Sun, G.; Zhao, Z. Y. Geochemical characteristics and hydrocarbon-generation potential of coal-bearing source rocks in the deep part of Panxie mining areaHuainan. *J. China Coal Soc.* **2020**, *45*, 731−739.
(13) Moore, T. A. Coalbed methane: a review. *Int. J. Coal Geol.* **2012**, *101*, 36−81.
(14) Scott, A. R.; Kaiser, W. R.; Ayers, J. W. B. Thermogenic and secondary biogenic gases, San Juan basin, Colorado and New Mexico−implications for coalbed gas producibility. *AAPG Bull.* **1994**, *78*, 1186−1209.
(15) Li, Y.; Tang, D. Z.; Yang, Y.; Hao, X.; Meng, Y. J. Distribution and genesis of stable carbon isotope in coalbed methane from the east margin of Ordos Basin. *Sci. China: Earth Sci.* **2014**, *57*, 1741−1748.
(16) Kotarba, M. J. Origin of natural gases in the Paleozoic-Mesozoic basement of the Polish Carpathian Foredeep. *Geol. Carpathica* **2012**, *63*, 307−318.
(17) Whiticar, M. J. Correlation of Natural Gases With Their Sources. In *The Petroleum System − From Source to Trap*, Magoon, L. B.; Dow, W. G., Eds.; AAPG: Tulsa, OK, 1994; pp 261−283.
(18) Zhang, H.; Cui, Y. C.; Tao, M. X.; Peng, G. L.; Jin, X. L.; Li, G. H. Evolution of the CBM reservoir-forming dynamic system with mixed secondary biogenic and thermogenic gases in the Huainan coalfield, China. *Chin. Sci. Bull.* **2005**, *50*, 30−39.
(19) Whiticar, M. J. A geochemial perspective of natural gas and atmospheric methane. *Org. Geochem.* **1990**, *16*, 531−547.
(20) Whiticar, M. J. Carbon and hydrogen isotope systematics of bacterial formation and oxidation of methane. *Chem. Geol.* **1999**, *161*, 291−314.
(21) Meng, Z.; Yan, J.; Li, G. Controls on Gas Content and Carbon Isotopic Abundance of Methane in Qinnan-East Coalbed Methane Block, Qinshui Basin, China. *Energy Fuels* **2017**, *31*, 1502−1511.
(22) Tao, M. X.; Shi, B. G.; Li, J. Y.; Wang, W. C.; Li, X. B.; Gao, B. Secondary biological coalbed gas in the Xinji area, Anhui province, China: Evidence from the geochemical features and secondary changes. *Int. J. Coal Geol.* **2007**, *71*, 358−370.
(23) Whiticar, M. J. Stable isotope geochemistry of coals, humic kerogens and related natural gases. *Int. J. Coal Geol.* **1996**, *32*, 191−215.
(24) Dai, J. X.; Shi, X.; Wei, Y. Z. Summary of the inorganic origin theory and the abiogenic gas pools(fields). *Acta Pet. Sin.* **2001**, *22*, 5−10.
(25) Rice, D. D. Composition and origins of coalbed gas. *AAPG Stud. Geol.* **1993**, *38*, 159−184.
(26) Smith, J. W.; Pallasser, R. J. Microbial origin of Australian coalbed methane. *AAPG Bull.* **1996**, *80*, 891−897.
(27) Kotarba, M. J. Composition and origin of coalbed gases in the Upper Silesian and Lublin basins, Poland. *Org. Geochem.* **2001**, *32*, 163−180.
(28) Zhang, K.; Meng, Z.; Wang, X. Distribution of methane carbon isotope and its significance on CBM accumulation of No. 2 coal seam in Yanchuannan CBM block, Ordos Basin, China. *J. Pet. Sci. Eng.* **2019**, *174*, 92−105.
(29) Liu, H. H.; Lan, T. H.; Hu, B. L.; Xue, J. H.; Xu, H. J.; Zhang, W. Y.; Ren, B.; Huang, Y. H. Geochemical characteristics and its origins of CBM in deep-seated coal seam around Panji mining area of Huainan. *J. China Coal Soc.* **2018**, *43*, 498−506.
(30) Ayers, W. B. Coalbed gas systems, resources, and production and a review of contrasting cases from the San Juan and Powder River basins. *AAPG Bull.* **2002**, *86*, 1853−1890.
(31) Zhan, R.; Zhang, W. Y.; Dou, X. Z. Tectonic Evolution and Coal Measures Natural Gas Reservoir in Huainan Coalfield. *Coal Geol. China* **2017**, *29*, 24−29.
(32) Zhang, X. J.; Tao, M. X.; Wang, W. C.; Ma, J. L.; Shi, Y. J. Geochemical behaviors of secondary biogas in Panji and Zhangji Coal Mines in Huainan coalfield. *Nat. Gas Ind.* **2008**, *28*, 34−38.
(33) Wei, Q.; Li, X. Q.; Zhang, J. Z.; Hu, B. L.; Zhu, W. W.; Liang, W. L.; Sun, K. X. Full-size pore structure characterization of deep-buried coals and its impact on methane adsorption capacity: A case study of the Shihezi Formation coals from the Panji Deep Area in Huainan Coalfield, Southern North China. *J. Pet. Sci. Eng.* **2019**, *173*, 975−989.
(34) Zhang, X. J.; Tao, M. X.; Xie, G. X.; Wang, Y. L.; Shi, B. G. Studies on resources significance and mixing proportion of secondary biogenic gas in coalbed gases, Huainan coalfield. *Acta Sediment. Sin.* **2007**, *25*, 314−318.
(35) Dai, J. X.; Qi, H. F.; Song, Y.; Guan, D. S. Composition and carbon isotope types of coalbed methane in China and their genesis and significance. *Sci. China* **1986**, *12*, 5−10.
(36) Qin, Y.; Tang, X. Y.; Ye, J. P. Stable carbon isotopic composition of coalbed methane in the Upper Paleozoic in North China and desorption-diffusion effect of coalbed methane. *Geol. J. Univ.* **1998**, *4*, 8−13.
(37) Li, Q. G.; Ju, Y. W.; Bao, Y.; Yan, Z. F.; Li, X. S.; Sun, Y. Composition, Origin, and Distribution of Coalbed Methane in the Huaibei Coalfield, China. *Energy Fuels* **2015**, *29*, 546−555.
(38) Bao, Y.; Wei, C.; Wang, C.; Li, L.; Sun, Y. Geochemical characteristics and identification of thermogenic CBM generated during the low and middle coalification stages. *Geochem. J.* **2013**, *47*, 451−458.
(39) Ge, T.; Chu, T. T.; Liu, G. J.; Fan, X.; Wu, D. Characteristics of hydrogen and oxygen isotopes of deep ground water in the Panxie mining area in Huainan Coalfield. *J. Univ. Sci. Technol. China* **2014**, *44*, 112−118.
(40) Zhang, L.; Qin, X. G.; Liu, J. Q.; Mu, Y.; An, S. Q.; Lu, C. H.; Chen, Y. C. Characters of hydrogen and oxygen isotopes of different water bodies in Huainan Coal Mining Area. *J. Jilin Univ.* **2015**, *45*, 1502−1514.
(41) Ao, W. H.; Huang, W. H.; Tang, X. Y.; Chen, P. Coal quality characteristics and distribution regularity in depth of Wangfenggang minefield, Huainan mining area. *Procedia Earth Planet. Sci.* **2011**, *3*, 123−130.
(42) Liu, H. H.; Hu, B. L.; Xu, H. J.; Zhang, W. Y.; Zheng, K. G.; Cheng, Q. Tectonic-thermal evolution characteristics of Permian mud shale in Panxie mining area of Huainan. *Nat. Gas Geol.* **2015**, *26*, 1696−1704.

https://doi.org/10.1021/acsomega.2c01227
ACS Omega 2022, 7, 17929−17940

(43) Qin, S. F.; Tang, X. Y.; Song, Y.; Wang, H. Y. Distribution and fractionation mechanism of stable carbon isotope of coalbed methane. *Sci. China Ser. D* **2006**, *49*, 1252−1258.
(44) Bi, B.; Chen, Y. C.; Xie, H.; An, S. K.; Xu, Y. F. Water inrush warning system of deep limestone in Panxie Mining Area based on multi-source data mining. *Coal Geol. Explor.* **2022**, *50*, 81−88.
(45) Scott, A. R. Hydrogeologic factors affecting gas content distribution in coal beds. *Int. J. Coal Geol.* **2002**, *50*, 363−387.
(46) Qin, S. F.; Song, Y.; Tang, X. Y.; Fu, G. Y. Effect of hydrodynamic force on carbon isotope of coalbed methane. *Nat. Gas Ind.* **2005**, *25*, 30−32.

https://doi.org/10.1021/acsomega.2c01227
ACS Omega 2022, 7, 17929−17940